

A method for determining neural connectivity and inferring the underlying network dynamics using extracellular spike recordings

Valeri A. Makarov^{a,*}, Fivos Panetsos^a, Oscar de Feo^b

^a *Neuroscience Laboratory, Department of Applied Mathematics, School of Optics, Universidad Complutense de Madrid, Avda. Arcos de Jalon s/n, 28037 Madrid, Spain*

^b *Laboratory of Nonlinear Systems, Swiss Federal Institute of Technology Lausanne; EPFL-IC-LANOS, CH-1015 Lausanne, Switzerland*

Received 11 October 2004; received in revised form 10 November 2004; accepted 12 November 2004

Abstract

In the present paper we propose a novel method for the identification and modeling of neural networks using extracellular spike recordings. We create a deterministic model of the effective network, whose dynamic behavior fits experimental data. The network obtained by our method includes explicit mathematical models of each of the spiking neurons and a description of the effective connectivity between them. Such a model allows us to study the properties of the neuron ensemble independently from the original data. It also permits to infer properties of the ensemble that cannot be directly obtained from the observed spike trains. The performance of the method is tested with spike trains artificially generated by a number of different neural networks.

© 2004 Elsevier B.V. All rights reserved.

Keywords: Neural circuits; Spike trains; Connectivity identification; Network modeling

1. Introduction

The qualitative and quantitative analysis of the spiking activity of individual neurons is a very valuable tool for the study of the dynamics and architecture of the neural networks in the central nervous system (Kandel et al., 2000; Moore et al., 1966; Perkel et al., 1967a). Nonetheless, such activity is not due to the sole intrinsic properties of the individual neural cells but it is mostly consequence of the direct influence of other neurons, from a few to hundreds of thousands, which in general leads to dynamical behaviors far beyond a simple combination of those of the isolated neurons. Although any behavior of a neural network depends on the interactions of a high number of neural cells, on their morphology and their entire interconnection pattern, usually we cannot record the activity of each one of these cells but rather we are restricted to a very limited sample of the neurons of the network whose properties we aim to capture. Moreover, deducing the effective

connectivity between neurons whose experimental spike trains are observed is of crucial importance in neuroscience: first for the correct interpretation of the electrophysiological activity of the involved neurons and neural networks, and, second and probably more important, for correctly relating the electrophysiological activity to the functional tasks accomplished by the network, being as simple as a response to a sensory stimulus or complex as interpreting a literature text. The above mentioned notion “effective connectivity” is defined as the simplest neuron-like circuit that would reproduce the same temporal relationships between neurons in a cell assembly as those observed experimentally (Aertsen and Preissl, 1991). In other words, by “effective” we mean any observable direct or indirect interaction between neurons that alters their firing activity. Summarizing, when dealing with multiunit extracellular recordings we have the following objectives: (i) inferring the effective connectivity and neuron properties of sub-networks (limiting to neurons experimentally available) and (ii) extrapolating the functionality of the “whole” from the properties of the collected and classified sub-networks.

* Corresponding author. Tel.: +34 91 394 6900; fax: +34 91 394 6885.
E-mail address: vmakarov@opt.ucm.es (V.A. Makarov).

To address these problems a common experimental approach is to use extracellular multiunit recordings. In this case spike trains (the time instants of spike occurrences, point events), in general, do not allow any direct insights about the subthreshold and/or intrinsic membrane dynamics of the neurons. Nevertheless, spike trains can be used to identify the functional characteristics and architecture of the neural network they originated from (e.g. Perkel et al., 1967b; Segundo, 2003). Though possible, identifying the effective neural circuits from the spike trains represents a very complex task even for a network of few neurons. The available mathematical methods result undersized with respect to the research exigencies, and the large majority of neurophysiologists restrict their study to the description of the neural activity by means of cross-correlograms (Perkel et al., 1967b), a tool widely understood but which provides very limited knowledge about the functional properties of the neural networks. For instance, in the case of neural ensembles of three or more neurons the cross-correlation may be easily fooled by the presence of indirect connections (via other neuron(s)), or also due to a common input.

Recently, more sophisticated statistical methods have been introduced for the identification of effective connectivity in relatively large neural networks. Nevertheless, to extract the interactions among neurophysiological data from two or more neural elements, or brain sites, all these methods always recur to the evaluation of some kind of covariance or correlation between the multiple signals. In fact, even the methods that go beyond simple correlation (e.g., regression analysis, principal components analysis and multidimensional scaling) conceptually embody the notion of co-variation in activity (Horwitz, 2003). In this framework a method based on linear partialization (conditional probability) in frequency domain has been proposed in (Brillinger et al., 1976; Dahlhaus et al., 1997; Rosenberg et al., 1989). Although this approach allows distinguishing direct from indirect (through other neurons) connections, it does not differentiate between excitatory and inhibitory synapses, a problem solved by Eichler et al. (2003) by adopting a similar approach based on partialization in time domain. Another approach, called partial directed coherence (e.g. Sameshima and Baccala, 1999), uses Granger causality (Granger, 1969) to expose the direction of information flow. Further two more methods: direct causality (Kaminski et al., 2001), and direct directed transfer function (Korzeniewska et al., 2003) have been introduced. These methods allow identifying the presence of feedback between two or more neurons, but coupling polarities are not directly accessible. Although these methods have been successfully applied on simulated networks of randomly spiking coupled neurons, their application to real data is basically limited because: (i) they do not allow resolving mutual couplings between neurons and/or do not distinguish the type of such couplings; (ii) as a rule their application assumes the use of relatively large spike trains with constant statistical properties, a condition difficult to be satisfied in the experiments; (iii) they usually fail when applied to excessively rhythmic neural assemblies, a rather

common situation which may just represent an objective of the research. An additional very important remark is that all these methods assume a stochastic nature of the spike trains generated by neurons. Consequently, no considerations are made about the dynamics of the involved neurons or about the nature of the intrinsic processes that are responsible for such behavior, with the consequent enormous difficulties in subsequent steps of the study: assigning of functional and/or neurochemical properties of the neurons, determination of anatomical correlates, etc. Furthermore, all these methods deal only with the connectivity patterns, i.e. only presence and sometime type and direction of the couplings between neurons can be estimated. No knowledge about absolute values of couplings or other parameters of the network can be drawn.

In contrast to a purely statistic approach, a deterministic one can be considered. The main advantage of deterministic methods is the use of mathematical models for inferring single neuron or neural network properties (indirect method) especially useful where direct observation of the neural dynamics (experimental procedures) is very difficult or even impossible. In general, in the literature, the indirect inference of network properties from models is approached in a very abstract manner, considering relatively simple, usually vaguely biophysically meaningful, neuron models (like phase oscillators (e.g. Ermentrout, 1982), Fitzhugh-Nagumo (FitzHugh, 1961), Plant (Plant, 1981), Hindmarsh-Rose (Hindmarsh and Rose, 1984), etc.) connected in networks which are either large and extremely regular (chains, rings, lattices, global or random couplings) or composed of only few (two) neurons. Alternatively, the Hodgkin–Huxley formalism (Hodgkin and Huxley, 1952) for modeling the dynamics of an individual neuron can be adopted. However, the need of a priori investigations of the channel dynamics of each particular neuron and the synaptic transduction properties, together with the computational complexity of its integration, restrict as well its use to the cases of very regular networks or of only a few neurons. Whilst these approaches allowed studying many phenomena experimentally observed in the central nervous system (like partial synchronization, phase or frequency locking, different types of waves, clustering, etc.), they lack direct biophysical interpretation and, the study of the dynamics of intermediate size networks, having biophysically supported effective connectivity patterns, is still a challenging problem. In this direction, a method for extracting a dynamical system out of the interspike intervals (ISIs) has been proposed (Racicot and Longtin, 1997; Sauer, 1994). This method allows concluding, for instance, about the possible chaotic nature of the spike timings of a neuron (e.g. Pavlov et al., 2001). Recently another approach taking into account the deterministic dynamics of a single neuron activity has been introduced (Paninski, 2004; Paninski et al., 2003; Pillow and Simoncelli, 2003). This approach provides a biophysically more realistic alternative to the models based on Poisson (stochastic) spike generation. It was shown that the leaky integrate and fire cell driven by a noisy stimulus demonstrates an adaptive behavior

similar to the effects observed in vivo and in vitro; spiking dynamics may account for changes observed in the receptive fields measured at different contrasts. However, these methods assume neurons to be isolated; hence, they do not provide insights about the neural network structure and its relationships with the observed dynamics.

Within the deterministic approach, here we propose a novel mathematical method for the identification of connectivity and modeling of neural networks using extracellular spike recordings. The aim is to obtain an inferable deterministic model of the neural ensemble, including interneuron connections. Such a model allows studying the properties of the network independently from the original data and also permits to infer dynamical properties that cannot be directly obtained from the observed spike trains. The mathematical algorithm has been implemented and a PC package is freely available (Makarov, 2004).

2. Materials and methods

2.1. Network identification and modeling

The method we propose is capable to analyze a set of experimentally recorded spike trains providing a mathematical model of interconnected spiking neurons that generates spike sequences like the experimental ones. Moreover, our method provides the effective architecture of the neural network including type, direction, and strength of the synapses. Once obtained, the deterministic model of the neural network will help us in interpreting both the dynamic behavior of the single neurons and their interactions, characteristics that, in general, cannot be directly obtained from the merely spike trains. For this reason our procedure is divided in two steps: (i) determination of a mathematical model of the neural network and the neurons that form it and (ii) the use of the mathematical model

to investigate the network dynamics and functionality. Let us now give an outline of the method, whilst the mathematical details are reported in Appendix A.

Having spike series of N neurons we assume a network composed of N interconnected dynamical systems, each of which describes the spiking behavior of one recorded neuron, i.e. we consider one dynamical system for each neuron. The behavior of each of the N dynamical systems is described by a set of differential equations that depend on a number of parameters unknown “a priori”. The connections between neurons are represented by a $N \times N$ matrix W whose elements w_{kn} are the weights of the synapses between the n -th and the k -th neurons, e.g. w_{12} represents the synaptic weight of the coupling directed from the presynaptic neuron 2 to the postsynaptic neuron 1. Schematically, it results in a graph whose N vertices represent the neurons, whose spike trains are experimentally observed, and the links between vertices correspond to effective synapses between the corresponding neurons, as illustrated in Fig. 1A. Then, the parameter values of the network model (the parameters of each one of the dynamical systems and among them the strengths and types of the synapses in the network) are determined from the spike trains by means of a minimization procedure.

Recently, Jolivet et al. (2004) shown that detailed conductance-based models (Hodgkin–Huxley type) can be well fitted by single-variable integrate-and-fire models. Accordingly, for each of the N interconnected dynamical systems we use the single-compartment leaky integrate-and-fire model (e.g. Stein, 1967):

$$C \frac{dV}{dt} = -G_L(V - V_L) + I^0 + I_{\text{syn}}(t), \quad (1)$$

where V is the neural membrane potential, C the membrane capacity, G_L and V_L are the conductance and the reversal potential of the leakage current, $I_{\text{syn}}(t)$ is the synaptic current induced by the spikes from the other neurons of the network,

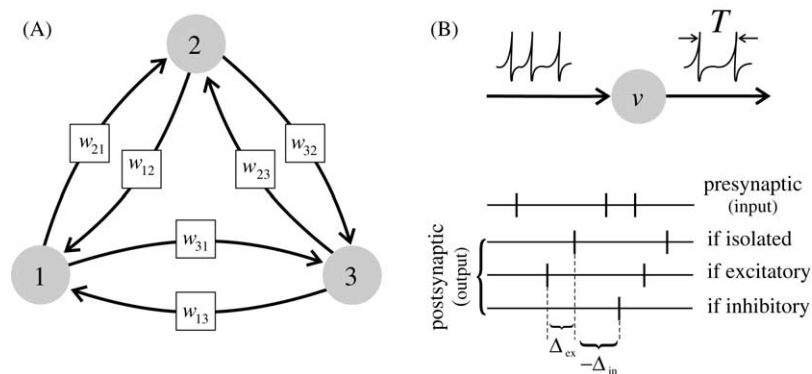


Fig. 1. Graphical representation of the network model. (A) Graph with N vertices (the case of three vertices is shown). Each vertex corresponds to a single neuron whose spike train is available experimentally. The intrinsic dynamics of a neuron is modeled by the single-compartment leaky integrate-and-fire model. Each neuron can receive synaptic input from $(N - 1)$ other neurons, and the links between vertices correspond to the (effective) synaptic connections between neurons. The connectivity matrix $\{w_{kn}\}$ defines the synaptic weights to be determined. Positive (negative) weight corresponds to excitatory (inhibitory) synapse, while zero corresponds to the absence of the synapse. (B) The input spike trains (the case of one train is shown) modify the neuron membrane potential and increase (decrease) for inhibitory (excitatory) synapses the ISIs of the neuron, with respect to its intrinsic firing.

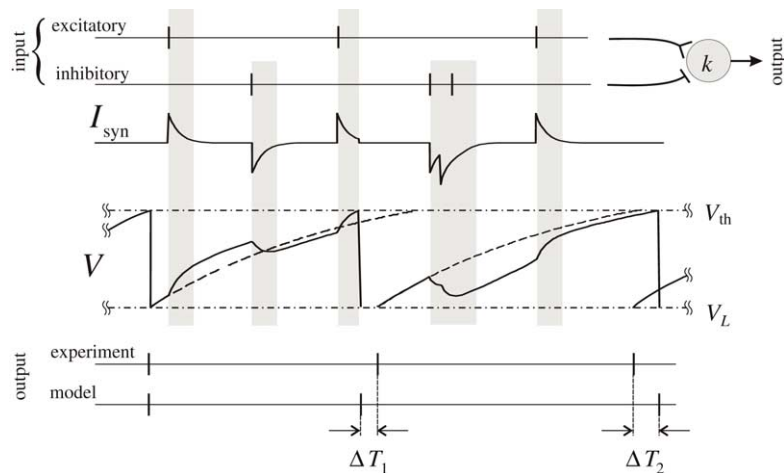


Fig. 2. Qualitative illustration of the working principle of the identification algorithm. A neuron, “ k ”, receives two synaptic inputs of different polarity, i.e. excitatory and inhibitory (two upper spike trains). Input spikes provoke postsynaptic current, I_{syn} ; the current associated with a single spike is modeled by an exponential function with amplitude and polarity defined by the corresponding entry of the connectivity matrix, W (in this case we have two components w_1 and w_2 for the two synapses). The time decays of the synaptic current, or duration of the synaptic transmission, are defined by two parameter λ_1 and λ_2 . The gray bars show time intervals when the membrane potential, V , is altered by the synaptic current and deviates (continuous line) from the intrinsic membrane dynamics (dashed line). When the membrane potential reaches the threshold, V_{th} , the modeled neuron fires a spike and V_{mem} is reset to the initial state, V_L . Accordingly, the parameter set $p = \{I^0, \tau, \lambda_1, \lambda_2, w_1, w_2\}$ defines uniquely the dynamics of the modeled neuron for a given input spike trains. Hence, the parameter values can be adjusted to minimize the sum of the squared differences (ΔT_i) between the experimentally observed firing of the neuron (“experimental output”) and the firing predicted by the model (“model output”). The resulting parameter set p^* gives the best (predictive) estimate of the intrinsic parameters and of the entries in the connectivity matrix corresponding to the modeled neuron.

and the constant current I^0 allows neurons to fire periodically when uncoupled. Whenever the membrane potential V reaches a threshold, V_{th} (about -50 mV) a spike is fired and V is instantaneously reset to the initial state, V_L . Hence, for $I^0 > G_L(V_{\text{th}} - V_L)$ the single neuron model (1) produces tonic spikes. Whilst, for non-spiking neurons, the resting membrane potential (usually about -60 mV) is $V^0 = V_L + I^0/G_L$.

Our procedure to adjust the parameters of the model uses the ISIs of the recorded spike trains. It relies on the general assumption that when a neuron receives an excitatory input it fires in advance with respect to its intrinsic firing interval and, consequently, it increases its firing rate. Inversely, it delays firing for inhibitory input with a consequent decrease in its firing rate (Fig. 1B). This is a general property of Type I membranes that have non-negative phase resetting curves (Ermentrout, 1996), which is indeed compatible with the leaky integrate-and-fire neuron model (van Vreeswijk et al., 1995). Type II neurons can have regions with negative phase resetting curves, for instance when undergoing a supercritical Hopf bifurcation (many membrane can be brought into this regime at high enough temperatures, but it is normally unusual) (Ermentrout, 1996).

The dynamic behavior of each neuron is determined by the parameters of each incoming synapse, by the incoming spiking activity and by the parameter values that determine its intrinsic behavior (leaky time and intrinsic spiking). Starting from arbitrarily assigned parameter values, we adjust them by means of a mean square method (Motulsky and Christopoulos, 2003) taking into account the differences between the predicted and measured spike trains.

Fig. 2 sketches the method working principle. We assume that the k -th neuron has two afferent synapses of different types, i.e. one excitatory and one inhibitory. For each one of the two synapses, an input spike induces an exponential current and the sum of them gives the postsynaptic current I_{syn} . The amplitude and the sign of the two components of the postsynaptic current are defined by the corresponding weights of the connectivity matrix, W ; in this case with only two synapses let us call them shortly w_1 and w_2 . Between each two spikes of the k -th neuron, in absence of external input, the membrane potential evolves according to its intrinsic dynamics (dashed line in Fig. 2, see also Appendix A). When external spikes income, the membrane potential deviates from its natural trajectory as highlighted in Fig. 2 and, every time it reaches the threshold V_{th} , the neuron fires a spike and V is reset to the initial state V_L . Given the input spike trains, the parameters of the equations of the model uniquely define the dynamics within two successive spikes of the neuron. At this point, keeping in mind that with this method we are interested in capturing the underlined dynamics of the network, we adjust the parameter values in order to minimize the sum of the squared differences between the experimental spike trains and the trains predicted by the model, i.e. the sum of the squared ΔT_i highlighted in Fig. 2. The set of the parameters corresponding to the global minimum of the squared sum (cost function) gives the best estimate of the components of the connectivity matrix and of the other parameters of the neurons in the modeled neural networks.

2.2. Use of the identified neural network model

Once a model of the whole neural network has been settled, i.e. all the parameters values of the equations (including the interconnections) have been determined, it can be mathematically investigated, independently from the original data, in order to assess the relationships between dynamical behavior and effective network architecture. The model of the network is functionally equivalent to the real one although the architectural differences between the real and modeled networks may be important. For example, the sequence of two or more interconnected neurons could be modeled by only one or a modeled neuron may send to postsynaptic neurons both excitatory and inhibitory connections.

A functionally meaningful neural network model fitting the observed data opens a broad variety of investigative possibilities. For example, one can study statistical properties of the model dynamics or bifurcations of the vector field and even collective chaotic behavior. As guidance, we report here two examples illustrating the kind of information that may be retrieved from the model, leaving the further exploitation of the modeling approach to the researchers.

It should be noted that, since we built a deterministic model, we can easily reverse the problem. Indeed, as soon as the parameter values of the model (i.e. connectivity matrix, decay scales, etc.) have been identified, the model equation can be numerically integrated (simulated), resorting for instance to one of the ODE integrators of Matlab[®], and the model spike trains can be obtained. Thought, since the commonly available simultaneous recordings are spike trains from few neurons despite the fact that they are part of larger neural circuits, a natural extension of the model is to add noise sources into Eq. (1) for modeling all unmeasured phenomena, including entrances from unobserved neurons and noising environment. In the simplest cases, white independent zero mean Gaussian processes (noise) can be used.

The simplest use of the model (through simulations) is the assessment of timing related properties. Simulations may be used to generate spike trains; then statistical properties (e.g. crosscorrelograms) of the model generated data can be computed and compared with those of the originally measured ones. This comparison can highlight, for instance, to which extent the observed statistical properties are related to the effective architecture, especially if the simulations have also been performed slightly modifying the identified parameters.

On the other hand, there are network properties which cannot be retrieved from the solely spike timings but which, on the contrary, may be inferred from the model. In the case when two tonic, approximately synchronous, spiking neurons are observed, usually the spike trains show very high regularity, their ISIs are practically constant and slightly varying with the synaptic input. Consequently, auto-correlation histograms will demonstrate equidistantly distributed peaks indicating the tonic spiking of both neurons and, at the same time, the cross-correlation will have at least one peak indicating the common behavior. However, the joint regularly spik-

ing of two neurons can be due to the dynamical behavior of three very different effective networks: (i) one of the neurons may not intrinsically fire at all and it produces tonic spikes due to input from the other neuron; (ii) alternatively, the firing frequencies of the two neurons are outcome of the collective dynamics (effective connectivity) and are, in general, different from their intrinsic frequencies; (iii) finally, no one of the two neurons is intrinsically spiking and their regular spiking is the result of the mutual effective interconnection. From the correlograms and other statistical methods it is not possible to distinguish which of these three cases is observed. On the contrary, this information is inferable from a simple mathematical analysis of the model: namely, if the identified parameter values of a neuron are so that $I^0/G_L(V_{th} - V_L) > 1$, then this neuron is intrinsically firing; otherwise the neuron fires due to the collective network dynamics.

2.3. Testing the method performance: generation of “experimental” spike trains

To verify our technique we used artificially generated spike trains, since the only way to judge the results of our method is to know all the properties of the network, especially the connectivity pattern. To generate the spike trains we consider five neural networks combining two essentially different kinds of neuron models: the probabilistic spike response model (SRM, Gerstner, 1995) and the deterministic model for regularly spiking (RS) neurons recently proposed by Izhikevich (2003). On one hand we chose the SRM because in the absence of couplings, such a neuron fires an irregular spike train with Poisson-like distribution of the ISIs, thus no assigned firing frequency exists. Consequently, it allows assessing the robustness of the method with respect to determinism of the modeled neuron. On the other side, the RS model has been chosen because it is a computationally efficient yet very plausible model of spiking neurons and permits to simulate a variety of behaviors of biological neurons, like spiking, bursting, chattering, frequency adaptation, etc. (Izhikevich, 2004). Since the RS model is strictly deterministic, to add variability to the dynamics and emulate the environmental fluctuations and/or the driving activity of other “unobserved” neurons, we introduce stochastic forces into the model equations. None of the two chosen neuron models belongs to the class of integrate-and-fire ones, since we want to assess the robustness of the proposed technique with respect to our most restricting hypothesis, i.e. the use of integrate-and-fire model. Equations and descriptions of the two models are briefly recalled in Appendix B.

Experiments 1–3 consider combinations of two RSM neurons: (1) unidirectional excitatory connection; (2) unidirectional inhibitory connection; (3) mutual inhibitory–excitatory loop. Despite that in theory there are $(2^3 + 1)$ cases, these three experiments practically cover all the possible two-neuron connections, since the other six are particular cases of these combinations. In experiment 4 we consider the mutual inhibitory–excitatory loop of two RS neurons; and in

experiment 5 we analyze the spikes generated from a classical three-neuron network formed by two interconnected RS and one SRM neuron. Experiment 6 assesses robustness of the method in respect to the amount of data (length of the available spike train recordings) and complexity of the underlying network (cases of three- and five-neuron networks are considered).

3. Results

First, the performance of the method is assessed on three neural networks of two probabilistic (SRM) neurons with low firing rates and one network of two tonic (RS) neurons; we generate experimental traces lasting 40 s for the SRM networks and 20 s for the RS network, thus having about 50–150 spikes for each experiment. Second, we use a mixed SRM-RS three-neuron network with experimental spike trains lasting 20 s. In each experiment we apply our method to identify

the connectivity pattern and intrinsic parameter values of the model of the neural network. Afterwards, we simulate the model at the identified parameters values. We compare the connectivity patterns (presence and type of the synapses), and we also crosscheck statistical properties, e.g. ISI and cross-correlation histograms, of modeled and “experimental” spike trains.

Finally (experiment 6), the robustness of the method is tested on two complex networks of three and five interconnected neurons. For each network we perform 100 Monte Carlo experiments varying the data segment length (duration of recording), and then we calculate the number of successful structural inferences as the number of correctly detected synapses divided by the number of possible couplings.

3.1. Experiment 1

Fig. 3 shows the results for the case of the unidirectional excitatory coupling. Here and further on, we use “V” and “T”-

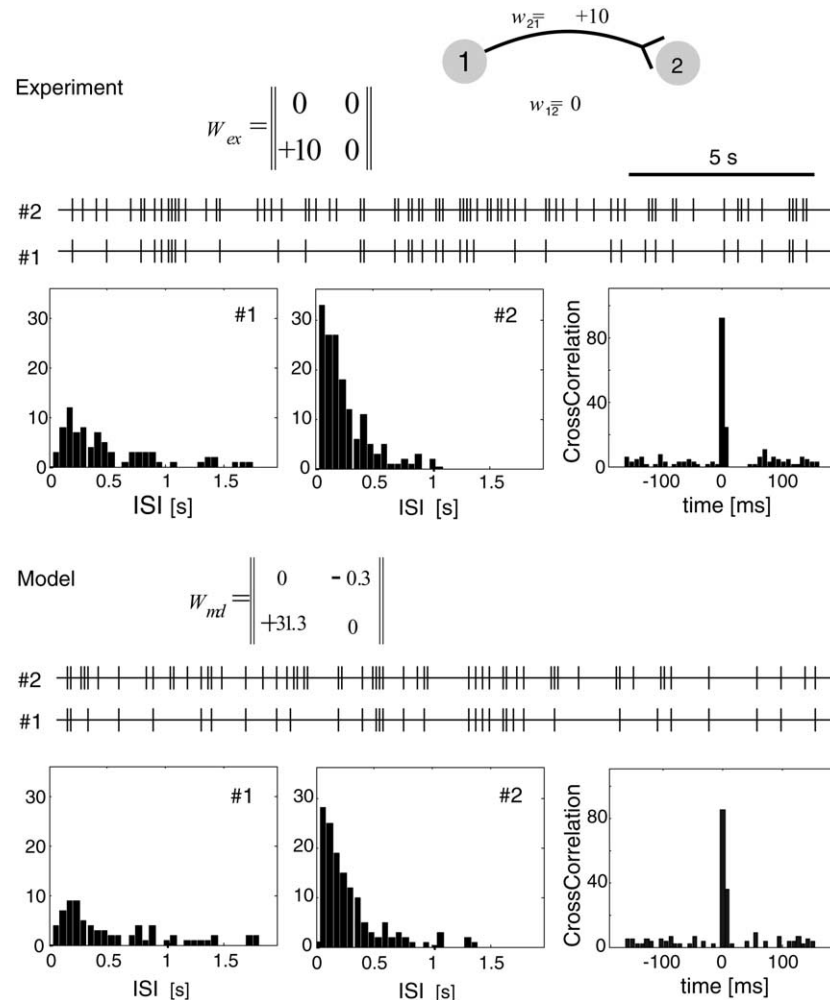


Fig. 3. Identification and modeling of a two-neuron network with unidirectional excitatory coupling between two SRM neurons. The upper part (“experiment”) shows the experimental spike trains and their ISI and cross-correlation histograms. The lower part (“model”) illustrates: the identified connectivity matrix, W_{md} , which captures correctly the experimental connectivity pattern (only presence, polarity and relative weights are comparable); and the modeled spike trains with their ISI and cross-correlation histograms, which are in a good accordance with their experimental counterparts.

like links ends to mark excitatory and inhibitory synapses respectively. The first neuron is autonomous; hence it fires irregularly with a very broad spectrum of ISIs. The firing of the second neuron, even though irregular, does depend on the spiking of the first neuron. The upper part of Fig. 3, marked as “experiment”, illustrates the experimental spike trains and the corresponding ISI and cross-correlation histograms. The cross-correlation histogram exhibits a high peak centered at a positive closed to zero value of time shift, suggesting the presence of coupling. The firing rate of both neurons is within the range of 0.5–50 Hz but, due to excitatory input, neuron 2 fires more frequently since the mean frequencies are 2 and 4 Hz for neurons 1 and 2, respectively. Neuron 2 may also produce bursts as a response to input spikes that strongly depolarize it. The blind use of the identification method detects correctly the presence (and strength) of the excitatory coupling ($w_{21} = +31.3$). It also estimates a negligible value (about 1% of the excitatory link) for the feedback coupling ($w_{12} = -0.3$). Indeed, further investigations show that this vanishing coupling is irrelevant for the dynamics of the network.

It should be noted that the “experimental” and identified coupling matrices can be compared only qualitatively as the absolute values of their entries are incommensurables. In fact, they refer to two completely different mathematical models. Moreover, even in the case where the same model has been used for both “experiment” and identification, the matrices are not “linearly” comparable since their elements are nonlinearly obtained upon the spike timings, e.g. for strong enough coupling strength the spiking rate may saturate or even decrease.

We performed a simulation using the model of the network we obtained and to which we have added a white noise. The lower part of Fig. 3, marked as “model”, reports the spike trains and the corresponding ISI and cross-correlation histograms of the model. The comparison of the upper and lower part of the figure highlights a good statistical agreement of the model with the experimental data. Indeed, as for the experimental data, neuron 1 fires with a strong variability of ISIs whilst, since the firing of the first neuron evokes spikes in second one, the ISI histogram of neuron 2 decays rapidly. Furthermore, the cross-correlation histogram exhibits a high

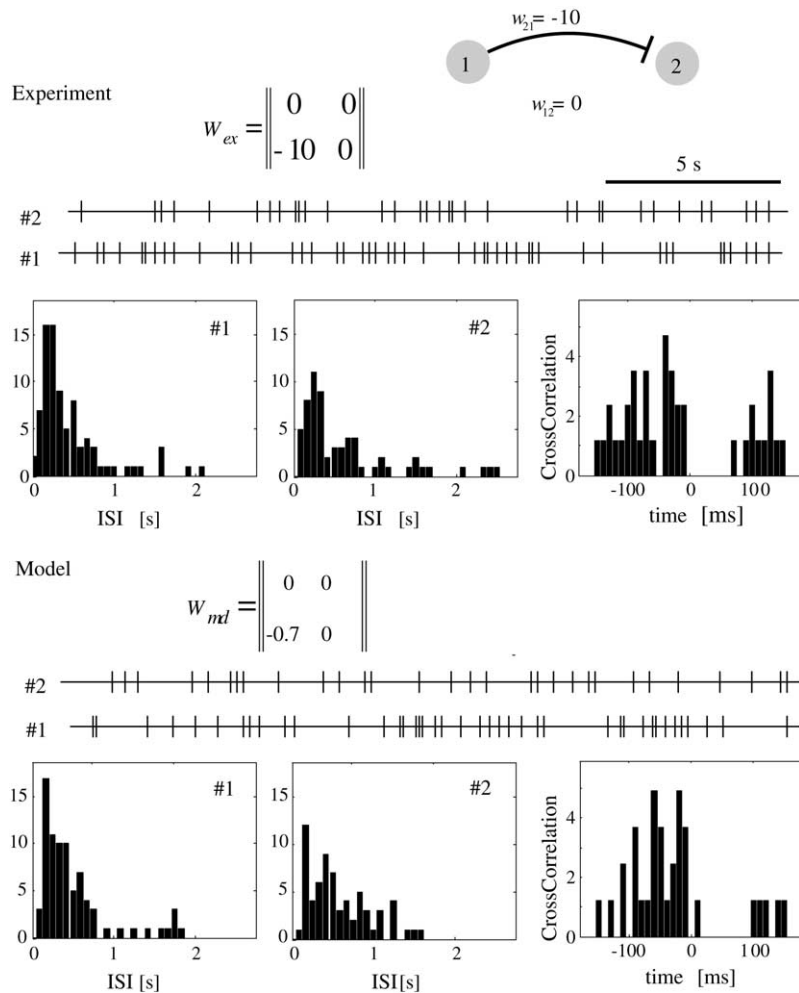


Fig. 4. Same as in Fig. 3 for the case of inhibitory coupling.

peak for small positive values of the time shift very similar to the one of the experimental data.

3.2. Experiment 2

Similarly to the first case, Fig. 4 shows the results for the case of inhibitory synapse. The inhibitory synapse induces two observable effects on the statistics: first of all the elongation of the ISI histogram of neuron 2, i.e. its mean firing frequency decreases to 1.6 Hz, and second, the emergence of a valley in the positive part of the cross-correlation histogram. Alike to the case of the excitatory synapse, the identification method provides the correct connectivity pattern, and the statistical properties of the model results very similar to those from the experiment, supporting further the potential of the method.

3.3. Experiment 3

Fig. 5 shows the results for the more complex case of two neurons forming an excitatory–inhibitory loop. In this case

the spike trains from the two neurons are not trivially interrelated. The presence of the excitatory synapse is pointed out by the experimental cross-correlation histogram, which shows a peak similar to that in Fig. 3 for the case of unidirectional coupling. However, the presence of an inhibitory synapse is not obvious as there is no pronounced difference between the histograms of Figs. 3 and 5. On the contrary, alike to the previous cases, the identification method provides the correct connectivity pattern, and the simulation of the network results in a satisfactory statistical accordance of experimental and model produced data.

3.4. Experiment 4

The last two-neuron network is composed by two tonic spiking neurons connected into an excitatory–inhibitory loop as shown in Fig. 6. The experimental spike trains and the results of their statistical analysis are shown in the upper part (“experiment”) of Fig. 6. The autocorrelations clearly demonstrates equidistantly distributed peaks representative of the tonic spiking of both neurons, whilst the peaks in the

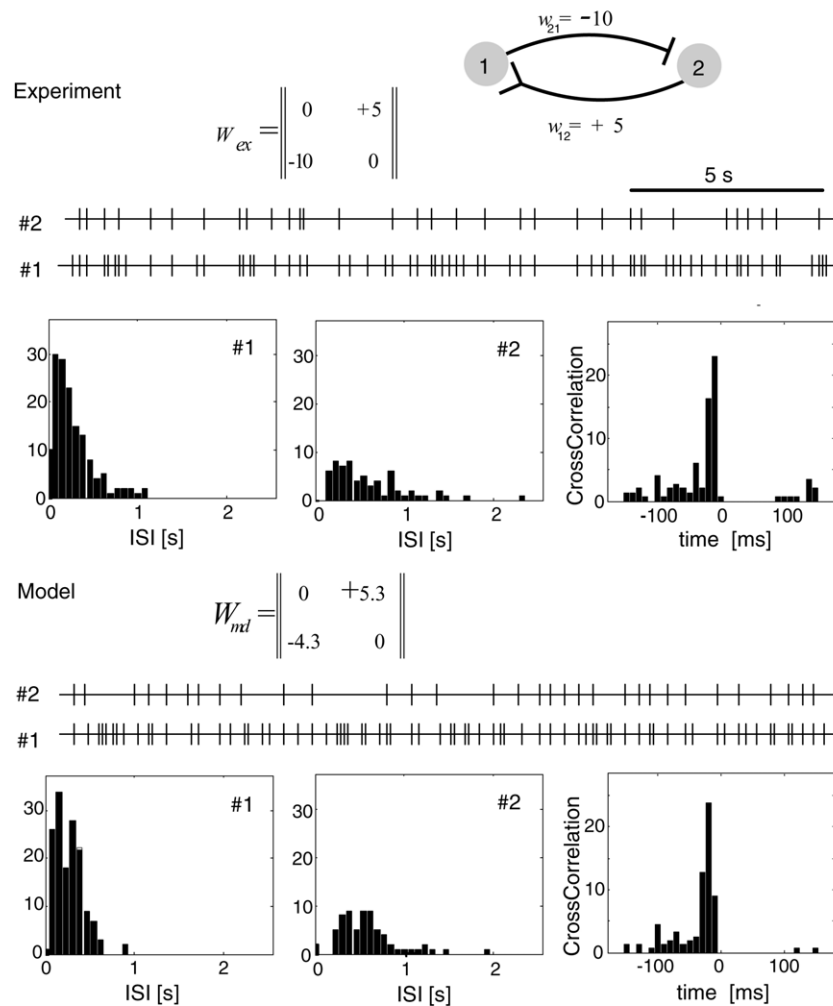


Fig. 5. Same as in Fig. 3 for the case of excitatory–inhibitory coupling loop.

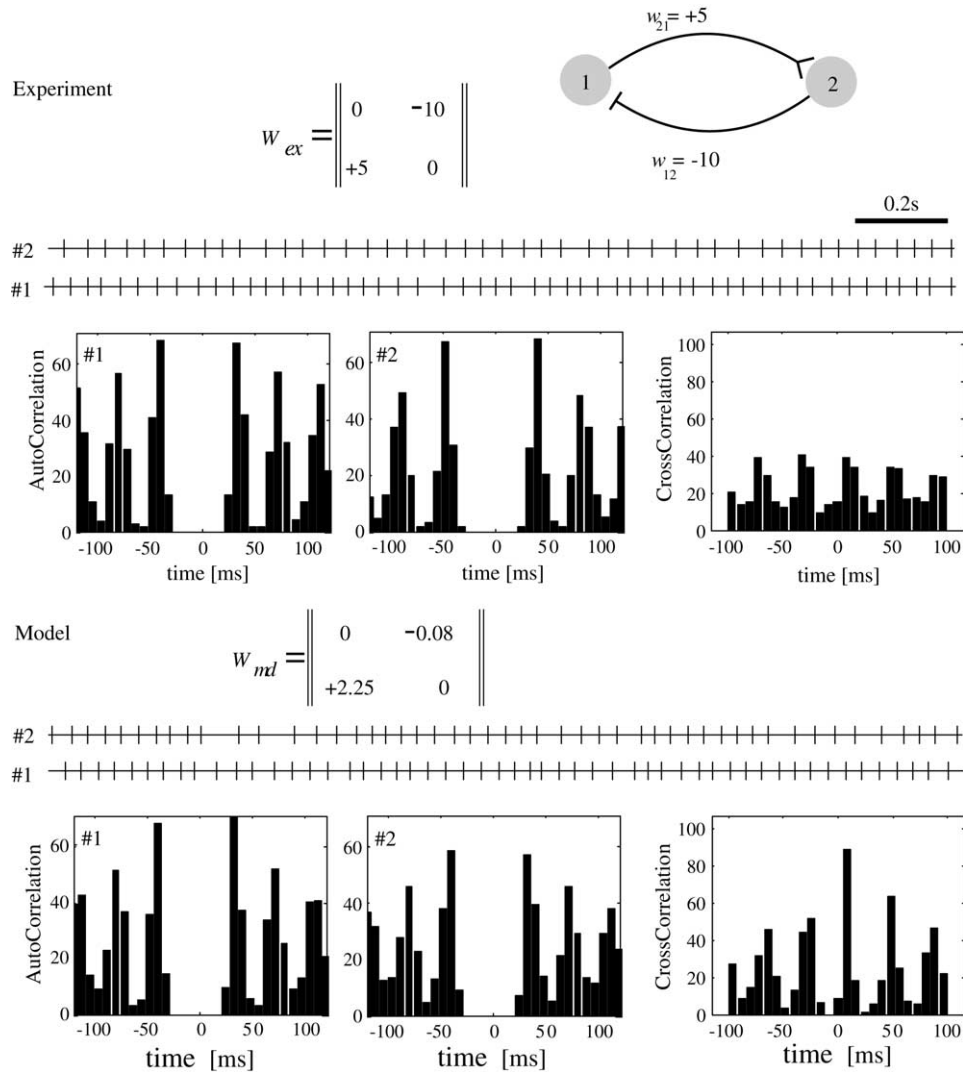


Fig. 6. Same as Fig. 3 for the case of a two-neuron network of mutually interconnected tonic spiking neurons (RS model).

cross-correlation highlight the presence of synaptic coupling. However, as in the previous experiment, the analysis of the histogram does not allow outlining the connectivity pattern neither allows drawing any conclusion about the intrinsic spiking nature of the two neurons. On the contrary, our identification method provides the correct connectivity pattern. Also the simulation of the modeled network provides results in a satisfactory statistical accordance with the experimental ones. As it can be seen, there is a good qualitative agreement between experimental and model cross-correlation histograms, though the former one has less pronounced peaks and the depression between peaks is not as strong as in the model histogram. This is due to the nature of the RS model we use for generating experimental spike trains which does not belong to the class of renewal models, i.e. its spiking shows adaptation phenomenon (Izhikevich, 2004). Consequently, the ISI following a short ISI tends to elongate, which in turn results in the fuzzy peaks of the experimental crosscorrelogram. Finally, the simulation of the two isolated (modeled)

neurons allows spotting exactly the intrinsic nature of both neurons as being regularly spiking, highlighting in this way the modeling ability of our identification technique.

3.5. Experiment 5

Fig. 7 summarizes the results obtained when applying the identification technique to a mixed RS-SRM three-neuron network. Considering the experimental data we observe that neuron 1 has a relatively high firing frequency and strong variability of ISIs and it fires in bursts when gets the excitatory input from the low rate irregularly firing neuron 2. On the other side, neuron 3 shows regular fast spiking activity. Note that this case has different feedback loops and indirect (via third neuron) connections, which makes problematic the study of the connectivity pattern by means of the conventional cross-correlation methods. However, in agreements to all the previous considered experiments, also for this harder case the application of our deterministic method leads to the iden-

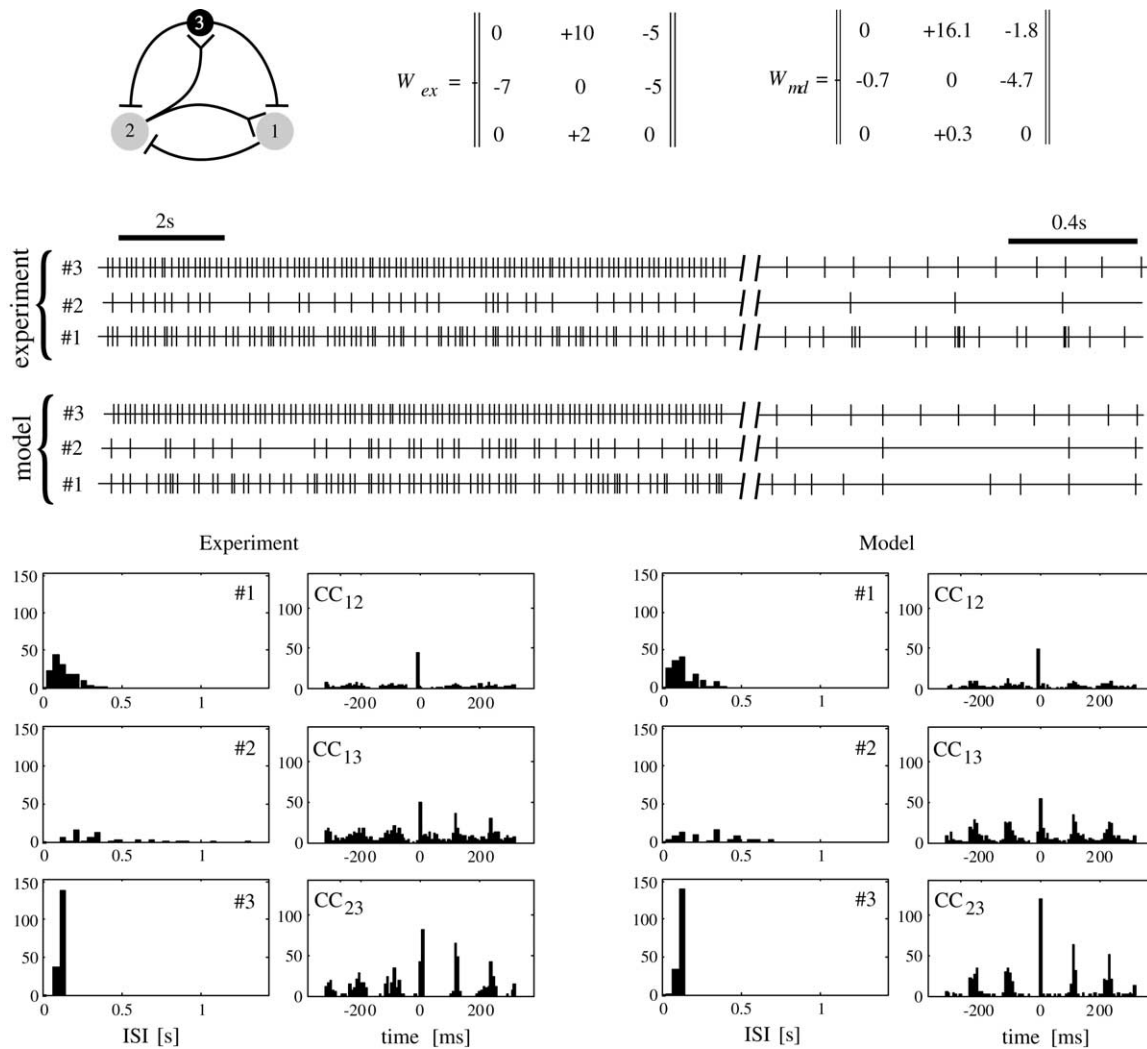


Fig. 7. Test of the method on a complex three-neuron network. Neurons 1 and 2 are modeled with SRM, while neuron 3 (SR model) fires tonic spikes with a high firing rate. The network includes different excitatory–inhibitory loops and indirect connections. The connectivity matrix W_{ex} is used for the generation of experimental spike trains. The outcome of the method application is the matrix W_{md} , which captures correctly the interneuron connectivity. Simulation of the identified neural network (model) shows a good statistical accordance with the experimental data.

tification of the correct connectivity pattern. Yet again, the simulation of the identified network provides results in a satisfactory statistical accordance with the experimental ones. The simulation of each one of the three neurons taken separately allows spotting the intrinsic regularly spiking nature of one of them, further highlighting the power of the proposed modeling technique.

3.6. Experiment 6

Fig. 8 summarizes the results of the robustness test. The network architecture, connectivity matrix and experimental spike trains for the case of the five-neuron network are shown in Fig. 8A, together with two representative examples of the connectivity matrix found during the identification using 20 and 60 s lasting spike trains, respectively. The matrix obtained for longer spike trains is structurally closer to the experimen-

tal one. In the case of three- (five-)neuron networks there exist 6 (20) couplings to be identified by the method. Fig. 8B shows (100 Monte Carlo simulations) the mean percentage of the correctly identified synapses as a function of the recording length. In both cases the method shows a good performance increasing with the amount of the data available for identification. In the case of the three-neuron network the method identifies correctly a 76.9% of the synapses with only spike trains lasting 10 s. The percentage reaches the 96.5% with 30 s of data and practically does not vary after this time interval (95.9% with 60 s). With the five-neuron network the performances are of 59.1%, 73.3% and 85.8%, respectively. Note that before identification each synapse in the connectivity pattern has “a priori” three equiprobable possibilities (it may be excitatory, inhibitory or null). Hence, a 50% of successes in the identification would mean a better performance than just a random assignation that in this case will

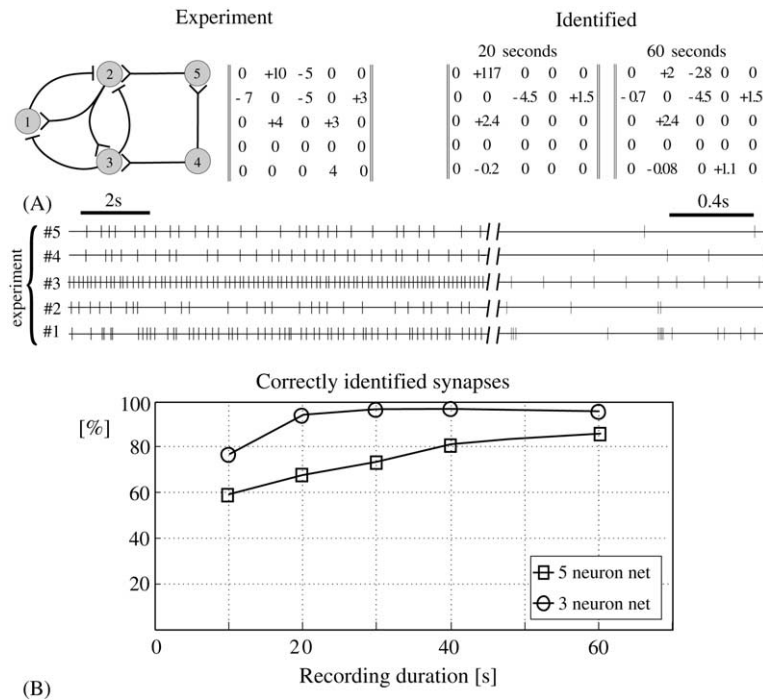


Fig. 8. Performance test of the network identification. (A) Results of a five-neuron network simulation and examples of connectivity matrices identified when using recording samples of two different durations: 20 and 60 s. (B) Mean percentage of correctly identified synapses as a function of the recording duration for the three- and five-neurons networks (in the former case experimental conditions are the same as in Fig. 7). Note that when counting successes we distinguish between inhibitory, null, and excitatory synapses. Thus even 50% of successful inferences correspond to a prediction much better than the one made by a random generator which would provide a 33% of success.

have 33% of success. As expected, the complexity of the network (number of involved neurons) decreases the method performance. For the same recording length a simpler network (three neurons) is identified better than the complex one (five neurons).

4. Discussion and conclusions

In the present paper we have proposed a novel deterministic method, which, for given spike trains of N neurons, allows obtaining a mathematical model describing both the architecture and the dynamical behavior of the underlined biological neural network. We have also shown that the obtained neural network model produces spike trains with statistical properties similar to those of the experimental data.

To model the network we use a set of interconnected integrate-and-fire neurons. All the parameter values necessary to univocally define the neural network, i.e. the matrix of the network connectivity, the synaptic time scales, and the intrinsic parameters of the neurons, are calculated from the recorded spike trains through an optimization procedure minimizing the difference between the predicted and the measured timings of spike episodes. Given the spike events, the identification of all the parameters is guaranteed by the decomposition of the fitting problem according to two nested independencies of the integrate-and-fire model: (i) the dy-

namical equation of each neuron remains independent from the others and (ii) the dynamics of each neuron within an interspike interval is independent from the dynamics within the other intervals.

The identification algorithm relies on the solely spike discharging times and any a priori knowledge of the parameter values, which may be provided by physiology, morphology, etc., can be included simply constraining to the given values (or ranges of values) the corresponding parameters, resulting also in a computational improvement. Furthermore, the method also allows considering bursting neurons simply recurring to a preprocessing of the spike trains: all the needed is to specify the minimal time interval for which two spikes are considered to be separated events and not belonging to a burst.

In order to assess the robustness of the method we generated “experimental” data sets considering neuron models denying the most restricting hypotheses on which the method trusts. Namely, we considered networks combining statistical responding (Gerstner, 1995) and not renewal regularly spiking (Izhikevich, 2003) neuron models. The former model denies the determinism, while the later one does not satisfied the resetting property of the neuron model we use in our method. Furthermore, the first five networks we considered collect the main difficulties reported in literature about the identification of the neural connectivity, like mutual and indirect couplings, inhibitory synapses, and excessively regular interspike inter-

vals, providing a reliable platform for the assessment of the identification technique.

In the first five experiments, we assessed separately the connectivity pattern identification and the modeling abilities of the method. For all the considered networks, the method provided the correct connectivity pattern. Simultaneously, with reference to the modeling issues, the simulation of the identified networks has provided spike trains with first order statistics in satisfactory accordance with the experimental ones. Also, for the more complex considered networks, the mathematical analysis of the identified model has correctly spotted intrinsic features of the isolated neurons which could not be inferred from the spike trains only, highlighting in this way the strength of the modeling technique. Finally (experiment 6), we checked the robustness of the method with respect to the amount of the available data (length of the spike trains) and the complexity of the underlying network applying identification of the connectivity pattern for data generated by relatively large networks with complex dynamics. The method showed a good performance that increased with the length of the data under study.

Concerning the identified connectivity pattern, it should be mentioned that the network connectivity obtained may differ from the anatomical network from which the data are observed (Aertsen and Preissl, 1991; Perkel et al., 1967a,b). Though, both of them are effectively equivalent for certain experimental conditions, i.e. they span the same dynamical behavior, which justifies the use of the term “effective synapse” or “effective network” we used through all the text to indicate the equivalent neural dynamical systems that could generate the observed data. The application of the method on artificial data allows measuring its potential and robustness within a handy environment; however, it is clearly not the aim and investigations on real data are underway.

Conversely to the descriptive nature of the statistical methods, which provides only a pattern of neural connectivity, the use of our deterministic approach offers a whole model of the neural network from which the experimental spikes are coming from. Such model includes the values of the parameters of the individual neurons (e.g. intrinsic firing frequency) and of the synapses between them. Consequently, we offer a powerful tool to approach the first of the two main steps in the study of neural circuits, i.e. inferring the dynamics of the neurons, and the effective connectivity of the network they belong to, from the recordings of the activity of a limited sample of neurons. This step is fundamental for addressing the second objective, i.e. extrapolating the functionality of the whole neural assembly from the properties of the analyzed sub-networks, the main aim of neuronal studies. Finally, it should be stressed that the obtained models can be subsequently studied independently from the experimental data; hence, information processing in neural circuits can be investigated and neural circuits can be classified depending on their architectures and dynamical properties.

Acknowledgments

This work was supported by the European Projects ROSANA (EU-IST-2001-34892), APEREST (EU-IST-2001-34893), Grants OFES-01.0456 and FIS 01/0822, and la Conserjería de Educación de la Comunidad de Madrid (V.A.M.).

Appendix A. Network model and parameter values adjusting procedure

Given N spike trains, we have a graph whose N vertices represent the neurons, and the links between vertices stand for the effective synapses between the corresponding neurons. The dynamics of each neuron (vertex in Fig. 1) is described by Eq. (1), driven by the external force (synaptic current) defined by the links structure. A rather accurate mathematical model of the synaptic current induced by a single spike is (Getting, 1989):

$$I_{\text{syn}}(t - t') = \Gamma \frac{1}{\lambda^d - \lambda^r} (e^{-(t-t')/\lambda^d} - e^{-(t-t')/\lambda^r}), \quad (\text{A.1})$$

where t' is the time instant when a spike from the presynaptic neuron arrives, Γ accounts for the synaptic strength and polarity (weight), and λ^d and λ^r are the time constants determining the decay and the rise time scales, respectively. For fast synapses the rise scale can be approximately set to zero, while for a slow synapse (e.g. GABA_A or NMDA) it is not vanishing although being usually less than the decay scale. Besides, from the modeling point of view λ^d plays a major role in determining the dynamics of the model network. Hence, to simplify the identification method, we can shorten the synaptic equation to:

$$I_{\text{syn}}(t - t') = \Gamma \frac{1}{\lambda^d} e^{-(t-t')/\lambda^d}. \quad (\text{A.2})$$

The total synaptic current for a neuron can be accounted by the sum over spikes generated by all the presynaptic neurons. The synaptic weights may be different among the synapses or be equal to zero, meaning in this case the absence of the synaptic coupling between certain neurons.

Let us consider one of the vertices-neurons, say the k -th and, to simplify notation, so forth we drop the index k in all variables and parameters. First, we introduce dimensionless membrane potential and time:

$$v = \frac{V - V_L}{V_{\text{th}} - V_L}, \quad t_{\text{new}} = \frac{t_{\text{old}}}{\theta}, \quad (\text{A.3})$$

where θ is a time scale constant that can be appropriately adjusted to account for neurons with largely different spike rates. Then, the evolution of the dimensionless membrane

potential, v , is written as

$$\dot{v} = -\frac{v}{\tau} + i^0 + \sum_{n=1, n \neq k}^N \left(w_n \sum_j \frac{1}{\lambda_n} \exp \left[-\frac{t - t_{nj}}{\lambda_n} \right] \right),$$

if $v = 1$ then $v = 0$ (A.4)

where the decay time scale, τ ; the constant current, i^0 ; synaptic time scales $\{\lambda_n\}$ and weights, $\{w_n\}$ are given by

$$\tau = \frac{C}{G_L \theta}, \quad i^0 = \frac{\theta I^0}{C(V_{tr} - V_L)}, \quad \lambda_n = \frac{\lambda_n^d}{\theta},$$

$$w_n = \frac{\Gamma_n}{C(V_{tr} - V_L)}. \quad (A.5)$$

The first sum in Eq. (A.4) is taken over all the presynaptic neurons, whilst the second one is taken over the spikes generated by these neurons between two consecutive spikes of neuron k . Note that all these parameters and the membrane potential are related to neuron k , so to have a complete set of equations we need to repeat the same procedure for all the other neurons. Summarizing, for N membrane potentials we have N equations as Eq. (A.4), each of which has $2N$ independent parameters: $p_k = (i_k^0, \tau_k, \lambda_{k1}, \dots, \lambda_{kN}, w_{k1}, \dots, w_{kN})$, being λ_{kk} and w_{kk} meaningless.

There are two nested independencies which allow the identification of the all parameter values. First, each Eq. (A.4) can be integrated independently from the others since the incoming spike time occurrences are known. This allows fitting each neuron to the data independently from the other neurons and their corresponding parameters. The second decomposition follows from the main property of integrate-and-fire models, namely the state variable, alias the membrane potential, is reset to a known value at every spike; this lets the dynamics of the neuron between two of its successive spikes be independent from its dynamics in the other ISIs.

Let us now denote by $\{T^i = t^{i+1} - t^i\}$ ($i = 1, 2, \dots, M$) the length of all the consecutive measured (experimental) ISIs of neuron k . Then, we classify all the spikes generated by the other neurons according to the ISI in which they fall, and we denote with $\{t_{nj}^i\}$ the relative (to t^i) times within this interval; where the index n indicates the number of the source neuron of the spike ($n \neq k$), index i stands for the number of the ISI of the k -th neuron, and index j for the number of input spike of neuron n falling inside the ISI i (Fig. A.1). Integrating Eq. (A.4) over each ISI, with boundary conditions $v(t^i) = 0$ and $v(t^i + T^i) = 1$, we obtain M equations as

$$(1 - e^{-\bar{T}^i/\tau})i^0\tau + \tau \sum_{n=1, n \neq k}^N \frac{w_n}{\tau - \lambda_n} \sum_j (e^{-(\bar{T}^i - t_{nj}^i)/\tau} - e^{-(\bar{T}^i - t_{nj}^i)/\lambda_n}) = 1. \quad (A.6)$$

where \bar{T}^i is the relative (to t^i) predicted by the model time occurrence of the $i + 1$ spike of neuron k .

This procedure is repeated for all the other neurons of the network, thus obtaining the equations completely defining

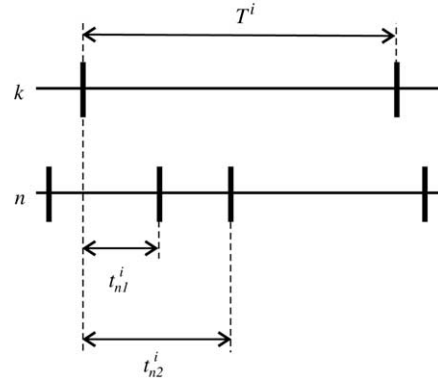


Fig. A.1. Illustration of relative time intervals between presynaptic and postsynaptic spikes; a fragment of two spike trains of postsynaptic neuron k , and presynaptic neuron n is shown. The postsynaptic neuron in its i -th ISI, T^i , receives two spikes with relative intervals t_{n1}^i and t_{n2}^i .

the connectivity matrix W and the other intrinsic parameters. We stress once more that, in general, the parameter values defining the dynamics of each neuron in the network (i.e., decay scale, constant current, and the synaptic constants) may differ amongst the neurons, thus accounting for the diversity of neurons and synapses.

Assuming that in the experiment we observed a sufficient number of spikes, so $M \gg 2N$, we can consider Eq. (A.6) as a nonlinear regression problem. Indeed, Eq. (A.6) can be presented in the form:

$$F(\bar{T}^i, \{t_{nj}^i\}, p) = 0 \quad (A.7)$$

where all input events $\{t_{nj}^i\}$ are known precisely (up to experimental precision). On the contrary, due to contamination by noise and inputs from unobserved neurons, the predicted relative time of spike occurrences, \bar{T}^i , may have a strong variability with respect to the measured values, T^i . Thus, we can consider T^i as a response vector in a nonlinear regression problem.

Eq. (A.7) are transcendental with respect to \bar{T}^i , so they can be inverted only numerically; moreover, they may have more than one solution. For a given parameter set p , we solve the ambiguity selecting the solution that corresponds to the minimal value of \bar{T}^i ; which physically means that a neuron fires a spike as soon as its membrane potential crosses the threshold. We present this solution as

$$\bar{T}^i = G(\{t_{nj}^i\}, p). \quad (A.8)$$

Then, comparing the predicted and measured spike time occurrences, we may formulate the following least square fitting problem (Fig. 2):

$$\min_p J = \sum_i (\Delta \bar{T}^i)^2 = \sum_i [T^i - G(\{t_{nj}^i\}, p)]^2, \quad (A.9)$$

whose solution provides the set of parameters p^* (including the connectivity matrix) that estimates the real parameter values.

Two main issues should be addressed when solving the regression problem (A.9) with real (physiological) data. First, the use of robust regression methods is preferable, e.g. nonlinear trimmed least squares estimator (Cizek, 2001). Indeed, the measured spike trains may be strongly corrupted by noise, because of the influence of “hidden” neurons or in consequence of wrong assignment during the spike-separation procedure (which is a complex problem as well; see for details e.g. (Harris et al., 2000)). Second, neuron bursting must be handled to avoid the deterioration of the method performance. Indeed, when a neuron produces a burst, a lot of very short “fake” ISIs appear. This would wrongly bias the solution of Eq. (A.6) to high values of I^0 , with the consequent underestimation of the connectivity weights (strong intrinsic high frequency firing). To avoid this problem we consider a burst of neuron k as a unique event when its parameters, and corresponding row of the connectivity matrix, are estimated. So the ISIs, $\{T^i\}$, are measured between the last spike of a burst and the next nearest spike.

Appendix B. Spike generation models

B.1. Spike response (probabilistic) model

The membrane potential of the k -th neuron is defined by the sum of two terms (Gerstner, 1995):

$$h_k(t) = h_k^{\text{ref}}(t - \hat{t}) + h_k^{\text{syn}}(t) \quad (\text{B.1})$$

where $h_k^{\text{ref}}(t - \hat{t})$ is a kernel describing the refractoriness of the neuron, \hat{t} the last firing time of the neuron, and $h_k^{\text{syn}}(t)$ describes the effect of the synaptic inputs from other neurons. The refractoriness is modeled as

$$h_k^{\text{ref}}(s) = \begin{cases} 0 & \text{for } s \leq 0, \\ -\infty & \text{for } 0 < s \leq s^{\text{ref}}, \\ \frac{\eta_0}{s^{\text{ref}} - s} & \text{for } s > s^{\text{ref}}, \end{cases} \quad (\text{B.2})$$

where s^{ref} is the absolute refractory period and η_0 accounts for the recovering scale. The change in the membrane potential at the soma due to a single incoming spike (postsynaptic potential) is described by the kernel (α -function):

$$\varepsilon(s) = \frac{s}{\tau_\varepsilon^2} \exp\left(-\frac{s}{\tau_\varepsilon}\right), \quad (\text{B.3})$$

where τ_ε is the synaptic decay constant. In order to calculate $h_k^{\text{syn}}(t)$, the contribution from a single spike is summed over all spikes of all presynaptic neurons:

$$h_k^{\text{syn}}(t) = \sum_{n=1, n \neq k}^N w_{kn} \int_0^\infty ds \varepsilon(s) \sum_j \delta(t - s - t_j^n) \quad (\text{B.4})$$

where $\{w_{kn}\}$ is the connectivity matrix, and $\{t_j^n\}$ are the firing times of neuron n .

Eqs. (B.1)–(B.4), together with the threshold θ , define a noise free model. In the presence of noise, the neuron may emit a spike even if the membrane potential has not reached the threshold or, on the other hand, it may not fire if the membrane potential crosses the threshold for a short time interval. A simple way to deal with noise is to introduce the probability of firing:

$$P = \frac{1}{2}(1 + \tanh[\beta(h(t) - \theta)]), \quad (\text{B.5})$$

where the parameter β determines the amount of internal noise. The probability for firing is equal to 1/2 for $h(t) = \theta$ and goes asymptotically to zero for $h(t) \rightarrow -\infty$ and to one for $h(t) \rightarrow +\infty$.

B.2. Regularly spiking neuron

The RS neuron model proposed by Izhikevich (2003) is

$$\begin{aligned} v' &= 0.04v^2 + 5v + 140 - u + I_{\text{dc}} + I_s + \zeta(t), \\ u' &= a(bv - u), \end{aligned} \quad (\text{B.6})$$

where time is scaled to ms, v is the membrane potential in mV, u represents a membrane recovery variable accounting for the activation of K^+ and inactivation of Na^+ ionic currents, while I_s and I_{dc} account for synaptic and dc currents, respectively. To account for variability in the spike trains we introduced the stochastic process, $\zeta(t)$, into the deterministic model. In our simulations we set parameters to their typical values: $a = 0.02$, $b = 0.27$, $c = -65$, and $d = 2$, ensuring high frequency (tonic) spiking with a spike frequency adaptation.

References

- Aertsen A, Preissl H. Dynamics of activity and connectivity in physiological neuronal networks. In: Schuster HG, editor. Nonlinear dynamics and neuronal networks. New York: VCH; 1991. p. 281–302.
- Brillinger DR, Bryant HL, Segundo JP. Identification of synaptic interactions. Biol Cybern 1976;22:213–28.
- Cizek P. Robust estimation in nonlinear regression models. Sonderforschungsbereich 2001;373:25 Humboldt Universitaet Berlin.
- Dahlhaus R, Eichler M, Sandkühler J. Identification of synaptic connections in neural ensembles by graphical models. J Neurosci Meth 1997;77:93–107.
- Eichler M, Dahlhaus R, Sandkühler J. Partial correlation analysis for the identification of synaptic connections. Biol Cybern 2003;89:289–302.
- Ermentrout GB. Asymptotic behavior of stationary homogeneous neuronal nets. Lecture notes in biomath. Berlin, New York: Springer; 1982. p. 45.
- Ermentrout GB. Type I membranes, phase resetting curves, and synchrony. Neural Comput 1996;8:979–1001.
- FitzHugh R. Impulses and physiological states in theoretical models of nerve membrane. Biophys J 1961;1:445–66.
- Gerstner W. Time structure of the activity in neural network models. Phys Rev E 1995;51:738–48.
- Getting PA. Reconstruction of small neural networks. In: Koch C, Segev I, editors. Methods in neuronal modeling: from synapses to networks. A Bradford Book. Cambridge: MIT Press; 1989. p. 171–94.
- Granger CWJ. Investigating causal relations by econometric models and cross-spectral methods. Econometrica 1969;37:424–38.

- Harris KD, Henze DA, Csicsvari J, Hirase H, Buzsaki G. Accuracy of tetrode spike separation as determined by simultaneous intracellular and extracellular measurements. *J Neurophysiol* 2000;84:401–14.
- Hindmarsh JL, Rose RM. A model of neuronal bursting using three coupled first order differential equations. *Proc R Soc London B* 1984;221:87–102.
- Hodgkin AL, Huxley AF. A quantitative description of membrane current and its application to conduction and excitation in nerve. *J Physiol* 1952;117:500–44.
- Horwitz B. The elusive concept of brain connectivity. *NeuroImage* 2003;19:466–70.
- Izhikevich EM. Simple model of spiking neurons. *IEEE Trans Neural Netw* 2003;14:1569–72.
- Izhikevich EM. Which model to use for cortical spiking neurons? *IEEE Trans Neural Netw* 2004;15:1063–70.
- Jolivet R, Lewis TJ, Gerstner W. Generalized integrate-and-fire models of neuronal activity approximate spike trains of a detailed model to a high degree of accuracy. *J Neurophysiol* 2004;92:959–76.
- Kaminski M, Ding M, Truccolo W, Bressler S. Evaluating causal relations in neural systems: Granger causality, directed transfer function and statistical assessment of significance. *Biol Cybern* 2001;85:145–57.
- Kandel ER, Schwartz JH, Jessell TM. Principles of neural science. 4th ed. New York: McGraw-Hill; 2000.
- Korzeniewska A, Manczak M, Kaminski M, Blinowska K, Kasicki S. Determination of information flow direction among brain structures by a modified directed transfer function (dDTF) method. *J Neurosci Meth* 2003;125:195–207.
- Makarov VA. Identification of Neural Connectivity and Modeling (IN-CAM) package is available at: <http://aperest.epfl.ch/docs/software.htm>, 2004.
- Moore GP, Perkel DP, Segundo JP. Statistical analysis and functional interpretation of neural spike data. *Annu Rev Physiol* 1966;28:493–522.
- Motulsky HJ, Christopoulos A. Fitting models to biological data using linear and nonlinear regression. A practical guide to curve fitting. San Diego: GraphPad Software Inc; 2003.
- Paninski L, Lau B, Reyes A. Noise-driven adaptation: in vitro and mathematical analysis. *Neurocomputing* 2003;52/54:877–83.
- Paninski L. Maximum likelihood estimation of cascade point-process neural encoding models. *Computation Neural Syst* 2004;15:243–62.
- Pavlov AN, Sosnovtseva OV, Moseckilde E, Anishchenko VS. Chaotic dynamics from interspike intervals. *Phys Rev E* 2001;63(5):36205.
- Perkel DH, Gerstein GL, Moore GP. Neuronal spike trains and stochastic point processes. I. The single spike train. *Biophys J* 1967a;7:391–418.
- Perkel DH, Gerstein GL, Moore GP. Neuronal spike trains and stochastic point processes. II. Simultaneous spike trains. *Biophys J* 1967b;7:419–40.
- Pillow JW, Simoncelli EP. Biases in white noise analysis due to non-Poisson spike generation. *Neurocomputing* 2003;52–54:109–15.
- Plant RE. Bifurcation and resonance in a model for bursting nerve cells. *J Math Biol* 1981;11:15–32.
- Racicot DM, Longtin A. Interspike interval attractors from chaotically driven neuron models. *Physica D* 1997;104:184–204.
- Rosenberg JR, Amjad AM, Breeze P, Brillinger DR, Halliday DM. The Fourier approach to the identification of functional coupling between neuronal spike trains. *Prog Biophys Mol Biol* 1989;53:1–31.
- Sameshima K, Baccala LA. Using partial directed coherence to describe neuronal ensemble interactions. *J Neurosci Meth* 1999;94:93–103.
- Sauer T. Reconstruction of dynamical systems from interspike intervals. *Phy Rev Lett* 1994;72:3811–4.
- Segundo JP. Nonlinear dynamics of point process systems and data. *Int J Bifurcat Chaos* 2003;13(8):2035–116.
- Stein RB. Some models of neuronal variability. *Biophys J* 1967;7:37–68.
- van Vreeswijk CA, Abbott LF, Ermentrout GB. Inhibition, not excitation, synchronizes coupled neurons. *J Comput Neurosci* 1995;1:303–13.